ELSEVIER

International Journal of Mass Spectrometry 206 (2001) 191–199

International Journal of Mass Spectrometry

Separation of neutral versus cationic dissociation processes in an ultracompact double time-of-flight spectrometer: first results on CH_3I

L. Lehr, R. Weinkauf*, E.W. Schlag

Institut für Physikalische und Theoretische Chemie der TU München, Lichtenbergstraβe 4, 85747 Garching, Germany

Received 14 June 2000, accepted 27 July 2000

Abstract

We present a simple experimental setup, which allows simultaneous detection and analysis of photoions and photoelectrons. In short, the apparatus is a hybrid of a time-of-flight mass spectrometer and a time-of-flight magnetic bottle photoelectron spectrometer. For ions and electrons the same field-free drift region as well as the same multichannel plate detector is used. Mass resolution $m/\Delta m$ is about 1000. Electron energy resolution ΔE decreases with absolute energy and is 50 meV at 0.5 eV. For lower electron energies the resolution is limited by the bandwidth of the 200 fs laser pulse. The apparatus is tested at the well-known $\tilde{A}$ state dynamics of methyl iodide by femtosecond pump–probe excitation and ionization. The observed fragment ions can have two different origins. They can be formed (1) either by parent cation photodissociation or (2) by ultrafast neutral fragmentation with subsequent fragment ionization by the intense probe laser. Because of the different ionization energies of CH_3I and iodine, neutral, and cationic dissociation pathways can be distinguished by means of electron energy analysis. This tool is very important for interpretation of mass and femtosecond laser pump–probe spectra of short-lived molecular systems. Because of the comparable detection probability for ions and electrons the apparatus would allow electron–ion coincidence measurements at kilohertz laser repetition rates. (Int J Mass Spectrom 206 (2001) 191–199) © 2001 Elsevier Science B.V.

Keywords: Time-of-flight mass spectrometry; Femtosecond laser excitation; Photoionization; Photofragmentation; Photoelectron spectroscopy

1. Introduction

The combination of resonant enhanced multiphoton ionization (REMPI) and mass spectrometry is a suitable tool for mass-selective optical spectroscopy and species-selective mass spectrometry [1–4]. In the early days of REMPI the fragmentation of aromatic molecules was found to occur by ionization of the parent molecule first and then by stepwise photodissociation to smaller fragment ions (ladder switch mechanism [5]). The advantage of this mechanism in combination with REMPI is the continuous steering of the degree of fragmentation by laser intensity from "no fragmentation" (soft ionization) to "complete fragmentation" (hard ionization). In the last 15 years, however, investigations with femtosecond and picosecond lasers discovered that in a variety of molecules and clusters the lifetimes of the intermediate states are short or ultrashort [6,7]. For a lot of small molecules

* E-mail: weinkauf@uni-duesseldorf.de

[1] Present address: Institut für Physikalische Chemie und Elektrochemie, Heinrich-Heine-Universität Düsseldorf, Universitätsstraβe 1, 40225 Düsseldorf

PII S1387-3806(00)00315-8

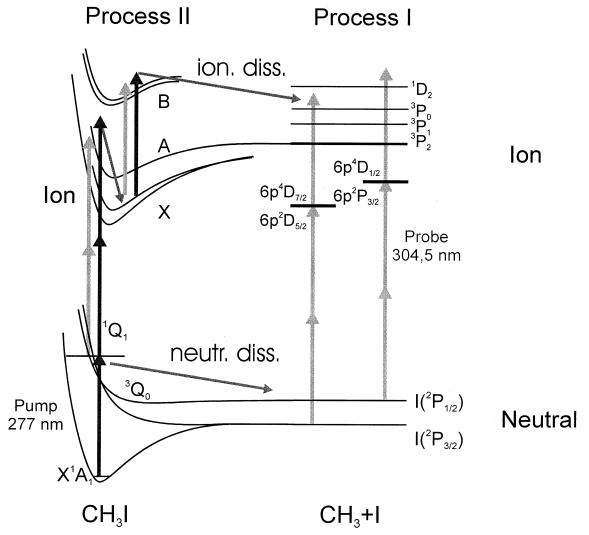

Fig. 1. Electronic state scheme of CH_3I and pump–probe scheme. Process I: after femtosecond pump excitation to the $\tilde{A}$ state ultrafast neutral dissociation occurs. CH_3 and I in the I(/2) and I(3/2) spin-orbit states are formed as fragments. At high laser intensity or by resonant excitation I or CH_3 fragments can be ionized by the probe laser. Process II: instead of dissociation because of the high laser intensity of the femtosecond pump or probe laser pulses also ionization of the parent molecule is possible. Ion photofragmentation then can be caused by either pump or probe laser absorption. The two fragment ion channels have to be distinguished in order obtain a complete picture of mechanism and dynamics of the neutral dissociation channel.

the fast excited state dynamics has been vastly investigated by various means of femtosecond pump–probe spectroscopy. In most cases to allow species and cluster size analysis, the dynamics is monitored by probe laser ionization and mass-selective detection. In principle, for investigation of dissociative states either the decrease of the parent ion or the appearance of the fragment ion as a function of the pump–probe delay can be detected. Only in few publications large molecules have been investigated mostly by nanosecond versus femtosecond one-color experiments [8,9,10]. For example by femtosecond laser pulse one-color REMPI and subsequent cation photodissociation nonergodic behavior in peptides has been found [8]. The ultrafast dissociation of the $\tilde{A}$ state of CH_3I has been extensively investigated [11–20]. The electronic state scheme including the two pathways for I^+ fragment ion formation are shown in Fig. 1. Resonant pump excitation of the parent molecule to the dissociative $\tilde{A}$ state leads to ultrafast fragmentation. Resonant or nonresonant probe laser ionization can form I^+ (or $CH_3{}^+$) (process I, Fig. 1). Because of the high pump laser intensity of the short pulses also formation of parent ions can occur. They can be photofragmented by the pump or the probe laser (process II, Fig. 1). Hence, we have two formation channels for fragment ions of same mass. Because the two channels are clearly involving different processes they carry different dynamics. A perfect discrimination is therefore essential for an analysis of the excited state dynamics but also for the interpretation of mass spectra. For aromats the fragmentation was easily attributed to cationic fragmentation because of the long lifetimes of the neutral intermediate states [5]. It is evident that detection of neutral fragments is possible by resonant ionization. By this for example the neutral dissociation of CH_3I to CH_3 and I has been detected [17]. Also in REMPI spectroscopy accidental coincidence of molecule and fragment absorption resonance may lead to fragment ionization [22]. In principle one can imagine two cases where femtosecond or nanosecond laser excitation may accidentally lead to ionization of neutral fragments. For small molecules fragmentation after resonant excitation typically leads to a large change of electronic properties. Hence the absorption of both fragments generally differs very much from the laser wavelength resonant to the parent molecule transition. For nanosecond laser excitation a nonresonant fragment ionization typically then fails because of the low laser intensity. By means of short-pulse lasers, however, the neutral fragments can also be ionized by nonresonant ionization due to the high laser intensity. Even worse, typically due to the high laser intensities of femtosecond lasers in pump–probe experiments ionization by $\lambda_{pump} + \lambda_{pump}$, $\lambda_{pump} + \lambda_{probe}$, and $\lambda_{probe} + \lambda_{probe}$ is possible. To distinguish all these processes i.e. to follow the pump–probe process an additional selectivity is necessary. For large molecules with an aromatic chromophore the absorption wavelength of the parent and the fragment molecule might be given by the chromophore and hence be very similar. Considering in addition the heating of the neutral

fragment by the dissociation process a nanosecond laser resonant with the parent molecule is resonant with the fragment and can efficiently ionize it. Such neutral fragmentation and neutral fragment ionization with nanosecond laser pulses has been observed for example for war agents [10]. Depending on the lifetime of the intermediate state femtosecond excitation might ionize fragments or intact molecules. Hence, in nanosecond and femtosecond laser ionization the origin of fragment ions can be twofold. They can be formed by (1) the neutral dissociation process followed by postionization and (2) the cation dissociation. The question is how the two fragment routes can be discriminated. A straightforward concept is the discrimination by energy release of the fragments. This is, however, only applicable to molecular systems where the neutral and cationic fragmentation channels are well known and differ much in fragment kinetic energy. This is for example the case for CH_3I where in the neutral a high energy and in the cation a low energy is released into the fragments [16]. For larger molecules this might fail because the energy is randomized and a small energy is transferred into the kinetic energy only. A more general means might be photoelectron spectroscopy (PES). Usually parent and fragment ionization energies differ significantly. For example by nanosecond laser REMPI, PES dissociation of a neutral intermediate state was detected by the appearance of the PE spectrum of the fragment [21]. For femtosecond laser excitation recording the photoelectrons in dependence of pump–probe delay would directly unravel the intermediate dissociation process. Such combination has been applied by several groups to monitor wave packet dynamics of molecules and clusters by PES [23–28]. For a detailed interpretation of dissociative processes, however, the ion mass and the corresponding electron energy is needed. Photoelectron–photoion coincidence spectroscopy is the perfect tool to correlate electron energy and ion mass [29–32]. Its application to femtosecond laser pump–probe spectroscopy became recently possible due to the high repetition rates of Ti:sapphire laser systems. For clusters it has been shown that complex neutral intermediate state dynamics can be projected into the photoelectron spectrum and directly correlated to the cluster size, i.e. mass [31,32]. Such an apparatus is typically a combination of two instruments mounted on opposite side of the common ion source, a mass spectrometer and a photoelectron spectrometer. Due to the complexity of this setup such measurements are still very sparse. Here we present a simple experimental setup, which also allows simultaneous detection and analysis of photoelectrons and photoions. The apparatus consists of a single ion source, a single drift region and a single multichannel plate (MCP) detector. Depending on the voltage applied at the ion source the apparatus is used as a linear time-of-flight mass spectrometer or a time-of-flight "magnetic bottle type" photoelectron spectrometer. Pulsed switch between the two modes in principle allows electron and ion detection for each pump–probe laser cycle up to kilohertz repetition rates. Because of the comparable detection probabilities for ions and electrons due to the "magnetic bottle" design coincidence measurements are also possible at kHz laser repetition rates. The apparatus is tested by two-color femtosecond pump–probe excitation and ionization of the well-known system methyl iodide [11–20].

2. Experiment

The apparatus combines a linear time-of-flight mass spectrometer with a time-of-flight magnetic bottle type [33–35] photoelectron spectrometer. Both spectrometers use the same ion source, the same field-free drift region and the same multichannel plate detector. The overall experimental setup is shown in Fig. 2. The apparatus consists of three vacuum chambers for different tasks. The first chamber is the inlet chamber containing a continuous valve and a skimmer. The second chamber contains the ion source and the strong magnet for the magnetic bottle used for electron collection. The third chamber contains the drift tube with a magnetic guiding field and the detector. The valve has an orifice of 50 μm and can be heated up to 450 K. The sample bottle is mounted outside the vacuum chamber and can be heated independently. It is the coldest point of the inlet

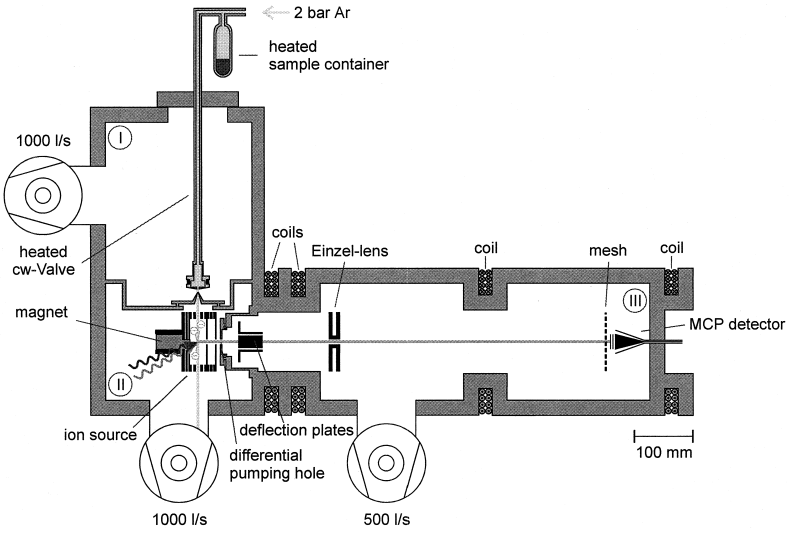

Fig. 2. Experimental setup of the hybrid of a linear time-of-flight mass spectrometer and a time-of-flight electron spectrometer. (I) Inlet chamber with valve and skimmer, (II) formation and extraction of ions and electrons, and (III) field-free drift region and ion and electron detection. Note that a switching of voltages allows first electron (photoelectron spectra) and then ion detection (mass spectra). A special concept allows electron and ion detection on the same microchannel plate detector.

system determining the total sample vapor pressure in the inlet system. A continuous inlet nozzle was chosen in order to allow high laser repetition rates up to1 kHz. The source chamber is pumped by a 1000 l/s turbomolecular pump in order to achieve collision-free conditions. For samples with low vapor pressure a pulsed valve with a repetition rate up to 250 Hz (General Valve Series 9) is used which can be heated up to 600 K. In this case the orifice is 150 μm and the sample is deposited directly in the valve itself. The supersonic expansion was skimmed 40 mm downstream with a heated skimmer of 1 mm diameter. The second chamber contains the ion source used simultaneously for the mass and photoelectron spectrometer. The laser crosses the molecular jet in the middle of the first field of a two-stage ion source perpendicular to the expansion. At small or zero electrode voltages first electrons are detected and afterwards the plates are pulsed to a high voltage (1500 and 1000 V) to accelerate the ions to the detector. For electron detection the ion source is set to zero or small acceleration or deceleration field in order to shift the electron energy into the energy range for optimized electron energy resolution [22]. For high electron collection efficiency a magnetic bottle time-of-flight photoelectron spectrometer was used [33–35]. The idea is to guide mostly all photoelectrons to the detector by an inhomogeneous magnetic field parallel to the flight axis. An electron emitted in an arbitrary direction is forced on a cyclic path around the symmetry center of the magnetic field. A divergent magnetic field acts like an electron mirror since the magnetic flux is an adiabatic invariant and therefore a velocity component parallel to the magnetic field forces the electron on spirals around the symmetry center. In the case of a velocity component in the direction of higher magnetic flux, the spirals get smaller and smaller until the whole translation energy is converted into rotational energy. At that point the electron is reflected and moves into the direction of lower magnetic flux maintaining the rotational direction. By this reflection a broadening of the flight time occurs due to the turnaround time between the photoelectrons emitted anti-parallel into and away from the turnaround point. This flight time broadening naturally results also in a energy broadening, i.e. a loss of resolution. Hence, for practical reasons a compromise has to be found between detection effi-

ciency and energy resolution. In our experiment the highly divergent magnetic field is formed by one permanent magnet (Sm_2Co_{17}) on the back of the ion source and coils in Helmholtz configuration. At the ionization site the magnetic field is about 700 mtesla and goes down to 1 mtesla at the detector. For this configuration the total collection efficiency is about 75% of all generated photoelectrons. For ion detection a pulsed electrical field is applied to the ion source, which is delayed by 1 to 2 μs. It accelerates the ions into the third chamber and to the ion detector. The two-field ion source is constructed in such a way that the space focus can be corrected to the second order [36]. The flight path was 50 cm long. Ions and electrons were detected on the same detector (see the following). The whole ion source is heated to reduce surface coverage and contact potentials. The ion source chamber is pumped by an 1000 l/s turbomolecular pump to maintain a pressure of 10^{-6} mbar. The overall flight path in the second vacuum chamber was kept as short as possible to avoid collisions. An orifice between chamber 2 and 3 acts as a differential pump stage. The flight tube is pumped by a turbomolecular pump of 500 L/s (pressure: 10^{-7} mbar). For the simultaneous acquisition of mass and photoelectron spectra the timing and the voltage of the pulsed ion extraction is crucial. Since all stray fields must be avoided during the photoelectron flight time the ion source is pulsed to positive voltage 1 to 2 μs after the laser pulse. During that time all photoelectrons have already reached the third chamber. The most crucial point is that the high voltage pulses have to start really at ground potential or accurately at the voltage needed for electron acceleration or deceleration. Even the smallest offset will cause flight time and therefore irreproducible energy shifts for the electrons. For the detection of charged particles a multichannel plate detector in Chevron configuration is used. Ions or electrons enter the detector by a gold mesh. The first MCP surface is set to +200 V. The voltage at each plate is between 800 and 900 V. The signal is coupled out via a capacity to the signal line, which is kept close to ground potential. The relatively slow electrons are accelerated to 200 eV in the detector, a voltage that allows high sensitivity for electrons [37]. The cations, which arrive with 1300 eV are decelerated to 1100 eV. The specification sheet shows that electron of 200 eV and small ions of 1100 eV energies have the same detection probability (about 30%–40% [37]). As a result of our timing scheme first the electrons arrive and then the ions. All measurable photoelectrons reach the detector within the first 2 μs and the whole photoelectron spectrum can be discriminated form even the fastest species (hydrogen) of the mass spectrum. For coincidence measurements a detection of electrons and ions by independent start and stop logics and time-to-amplitude as well as analog-to-digital converters is recommended. They only allow single particle detection, a typical condition for coincidence measurements, but allow very high repetition rates. In our setup the signal was split with an 50 Ω, 6 dB power divider (SUHNER). The first two microseconds the photoelectron spectrum, were measured with a single particle counting system (Stanford Research SRS430) and the full time window was recorded by an oscilloscope (LeCroy IC 9384) in peak detection mode to acquire the ion mass spectrum. The multichannel scaler is specialized for single particle detection at high repetition rates. A trigger signal starts the acquisition of one record consisting of several time bins with 5 ns time duration. The number of signal pulses counted during each time bin is stored in a memory. Each new trigger starts a record whose data is added to the bin-by-bin accumulation of all previous records. Energy resolution of the photoelectron spectrometer depends on the overall kinetic energy and is for example 49 meV for 0.5 eV and 65 meV for 1 eV photoelectron kinetic energy. For electrons of low kinetic energy resolution is limited by the bandwidth of the laser. For high energy electrons resolution is limited by the time resolution of the particle counting system. The oscilloscope has a data acquisition rate of 100 megasamples/second: MS/s and therefore a mass spectrum of 20 μs ca be recorded in 1 ns intervals. This time resolution does not significantly affect the mass resolution $m/\Delta m$of 1000. The laser system used for the experiments is a commercially available femtosecond laser system consisting of an argon–ion pumped Ti:sapphire oscillator (Coherent Mira Basic), a regenerative amplifier

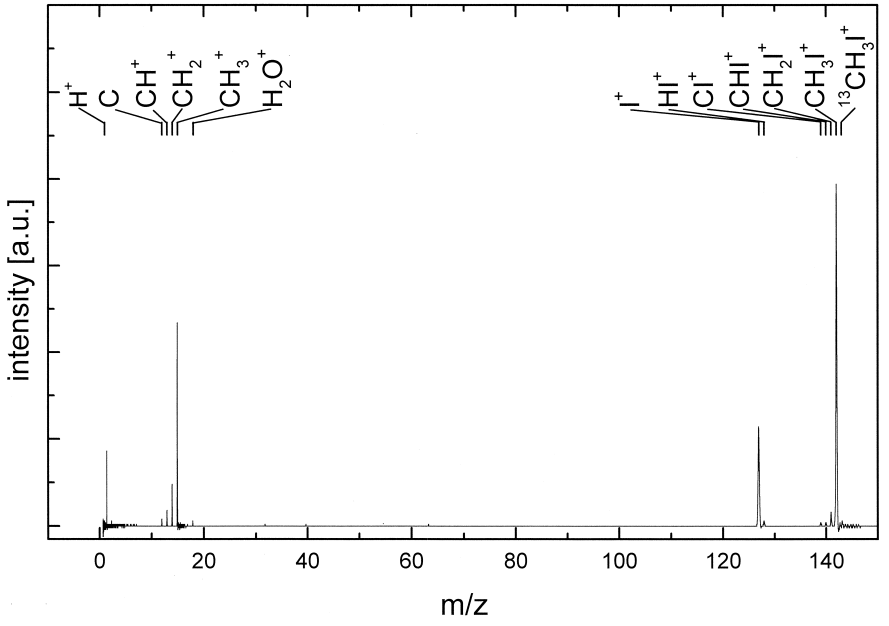

Fig. 3. One- color fs REMPI mass spectrum of CH_3I taken with a laser wavelength of 240 nm. Beside the parent cation also fragment ions of CH_3 and I are present. According to Fig. 1 they could in principal have neutral or ionic precursors. Mass resolution $m/\Delta m$ is about 1000.

(Spectra Physics Superspitfire) pumped by an Nd: YLF Laser (Spectra Physics Supermerlin) followed by a multipass amplifier. The pulses of the fundamental of 790 nm have a pulse duration of about 80 fs and are afterwards frequency converted by a parametric generator (Light Conversion TOPAS), mixed and frequency doubled. The final ultraviolet laser pulses are tunable between 230 and 280 nm and have typical energies of up to 50 μJ per pulse. The pulse duration in the UV is about 200 fs as measured directly in the supersonic expansion via nonresonant two-photon ionization of furane.

3. Experimental results and discussion

Fig. 3 shows a typical femtosecond laser pulse mass spectrum of methyl iodide obtained by the apparatus described above. The ionization wavelength for two photon ionization was 240 nm and the pulses had an energy of 8 μJ. By this laser wavelength the well-known ultrashort-lived $\tilde{A}$ state of CH_3I is excited [11–20]. The presence of the intact parent cation in the mass spectrum indicates that the laser excitation rate into ionization can efficiently compete with dissociation. Also fragmentation to CH_3^+ and I^+ ions takes place and even pure carbon ions can be found. As pointed out in the introduction (see Fig. 1) from the mass spectrum alone it cannot be figured out whether the fragment ions are (1) due to neutral fragmentation and subsequent nonresonant fragment ionization during the laser pulse or (2) due to ionization of the parent cation and subsequent photodissociation. The latter process can lead to the two fragment channels $CH_3 + I^+$ and $CH_3^+ + I$ [38]. In Fig. 4(a) the one color REMPI-PE spectrum of CH_3I taken at $\lambda = 240$ nm, corresponding to the mass spectrum above (Fig. 3), is shown. The resolution is below 50 meV for low-energetic electrons and is essentially given by the femtosecond laser bandwidth. The origins of the two spin-orbit components of the cation ground state are by far predominant and clearly separated by about 620 meV ($\Delta E_{SO} = 626.1$ meV [39]). The intensity of the two spin-orbit components is similar (peak area) indicating that the intermediate

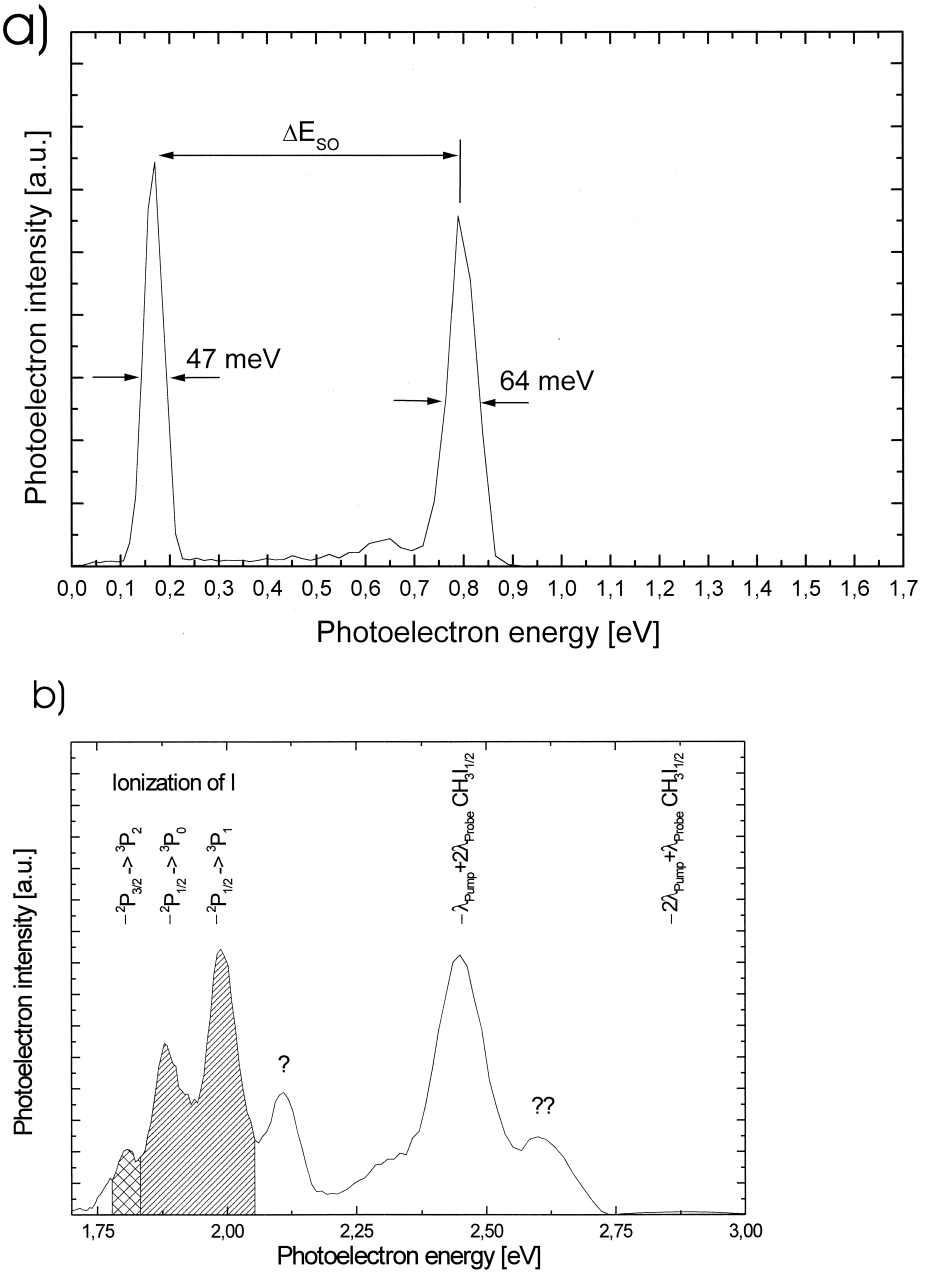

Fig. 4. (a) One-color two-photon REMPI-PE spectrum of CH_3I (λ = 240 nm): The origins of the two spin-orbit components of the cation ground state of CH_3I are by far predominant and clearly separated (ΔE_{SO} = 626 meV). Note the small intensity of vibrational features in the spectrum. The lack of photoelectrons from fragments shows that in one-photon REMPI with 200 fs laser pulse excitation all fragments are formed by cation fragmentation (process II in Fig. 1). The resolution is below 50 meV for low-energetic electrons and is essentially given by the femtosecond laser bandwidth. (b) Two-color two-photon REMPI-PE spectrum of CH_3I (λ_{pump} = 277 nm, λ_{probe} = 304.5 nm) recorded with a pump–probe delay of 100 fs: beside the two spin-orbit components due to ionization of the intact parent molecule ($\lambda_{pump} + 2\lambda_{probe}$ and $3\lambda_{probe}$) also structures due to pump laser ionization of the neutral fragments I(3/2) and I(1/2) appear (process I in Fig. 1). Recording of the electrons from ionization of the neutral I would allow to follow the intermediate state dynamics of CH_3I independently for the two channels I(3/2) and I(1/2). This dynamics will be published in a separate article. The peaks signed by question marks are due to the probe laser alone but cannot be assigned.

$\tilde{A}$ state does not provide a preference for ionization to one of the two spin-orbit states of the cation ground state *X*. Please note the nearly complete lack of vibrational features in the spectrum. This is in surprising contrast to the one-color two-photon REMPI-PE spectra of Fischer and co-workers [25] and might be due to the higher photon energy or the higher laser intensity in our experiment, providing a larger optical pumping rate. This cannot be clarified easily. On one hand the strong dependence on pump laser wavelength observed in the work of Fischer and co-workers favors [25] the explanation that the difference might be caused by our wavelength of 240 nm. Fisher and co-workers even found that a change of 1.5 nm changed considerably the vibrational cation ground state population. On the other hand the complete lack of photoelectrons from fragments shows that in one-color REMPI with 200 fs laser pulse excitation the optical pumping rate is larger than the dissociation rate and all fragments are formed by photodissociation of the parent cation. This is a surprising result, because Zewail and co-workers [14–16] find a lifetime of about 140 fs for the long-lived component, a time still within our laser pulse width. Hence we expect to see at least a small PE contribution by nonresonant ionization of I. The fact that no vibrational activity in the PE spectrum [Fig. 4(a)] is found indicates that at the laser intensity used the optical pumping rate is so high, that neutral dissociation is mostly avoided. The complete lack of photoelectrons [Fig. 4(a)] from neutral fragment ionization by nonresonant three photon ionization shows that under these conditions fragment ions are only formed via the cation pathway (process II, Fig 1). Due to the known cation dissociation energetics [38], the photodissociation presumably involves the $\tilde{B}$ state [39]. In case of the typical two-color pump–probe scheme used in femtosecond spectroscopy the situation is much more complicated because all multiphoton combinations of λ_{pump} and λ_{probe} are possible. However, usually only the signal stemming from the sequence λ_{pump} and then λ_{probe} is of interest. In our experiment the pump wavelength λ_{pump} is set to 277 nm which excites to the dissociative A state region into the $^3Q_0$ state. At this wavelength two-photon REMPI with λ_{pump} is impossible. The probe wavelength λ_{probe} was set to 304.5 nm to be resonant with a 2 + 1 REMPI of the I fragment. According to previous results of Zewail and co-workers [16] the I fragment should appear with the delay caused by the dissociation dynamics. In Fig. 4(b) a two-color two-photon REMPI-PE spectrum of CH_3I recorded with a pump–probe delay of 100 fs is shown. Multiphoton ionization of the intact parent molecule ($3\lambda_{probe}$ and $\lambda_{pump} + 2\lambda_{probe}$) is observed. The peaks signed by question mark are due to probe laser excitation only but cannot be assigned. At the left-hand side structures due to ionization of the neutral I fragment appear, which are due to their energy attribute to the pump–probe signal excitation to $\tilde{A}$, dissociation and ionization of neutral I. It is necessary to understand that I can be formed in the ground state 3/2 and in the 1/2 spin-orbit component. The 1/2 component is predominant. The three transitions $^3P_{3/2} \rightarrow {}^2P_2$, $^2P_{1/2} \rightarrow {}^3P_1$ and $^2P_{1/2} \rightarrow {}^3P_1$ to the three cation states of I^+ are found. The appearance of these peaks shows clearly that the neutral formation route for I^+ production is now active. By the well separated energies in the REMPI-PES the two intermediate dissociation channels leading to neutral I(1/2) and I(3/2) products can be separated. Recording of the electrons from ionization of the neutral I in dependence on pump–probe delay would allow to follow the intermediate state dynamics of CH_3I. The new option here is now that a distinction between the dynamics leading to the two products I(1/2) and I(3/2) is possible. This simple two-color experiment shows that the fragment ion signal is a superposition of ion dissociation and neutral dissociation with postionization. A detailed PES intensity measurement would give the percentage of neutral versus cation fragmentation. Both channels are different and show different dynamics. Recording the fragment cation intensity alone in dependence of pump probe delay by no means would reflect the dynamics of the neutral excited state. By recording the $^3P_{3/2} \rightarrow {}^2P_2$ and $^2P_{1/2} \rightarrow {}^3P_1$ transitions in dependence of pump–probe delay the detailed dynamics of the two decay possibilities of the $^3Q_1$ state can be investigated. This ultrafast dynamics will be published in detail in a separate article.

4. Conclusion

By means of electron energy analysis neutral and cationic dissociation pathways in CH_3I can be distinguished due to the different ionization energies of the molecule CH_3I and the neutral iodine. "Our results confirm the simultaneous presence of neutral and cationic fragment channels." Although this example is somewhat artificial it shows that REMPI-PES can provide additional detailed information about dissociation pathways, which might be important for the interpretation of pump–probe or mass spectra. The occurrence of neutral and ionic pathways for fragment ions is a general problem and might affect all femtosecond pump–probe experiments. Especially photoion photoelectron coincidence measurements might be very important for femtosecond laser pulse excitations of a variety of short-lived molecular and cluster systems in order not only to detect the presence of neutral fragment channels but also to correlate them directly to mass and dynamics.

Acknowledgements

Financial support from the Deutsche Forschungsgemeinschaft and the Fond der Chemischen Industrie is gratefully acknowledged.

References

[1] U. Boesl, H.J. Neusser, E.W. Schlag, Z. Naturforsch. 33a (1978) 1546.
[2] U. Boesl, R. Weinkauf, C. Weikhardt, E.W. Schlag, Int. J. Mass Spectrom. Ion Processes 131 (1994) 87.
[3] U. Boesl, R. Zimmermann, C. Weikhardt, D. Lenoir, K.-W. Schramm, A. Kettrup, E.W. Schlag, Chemosphere 29 (1994) 1429.
[4] C. Weikhardt, F. Moritz, J. Grotemeyer, Mass Spectrom. Rev. 15 (1996) 139.
[5] U. Boesl, H.J. Neusser, E.W. Schlag, Chem. Phys. Lett. 87 (1982) 1.
[6] Femtochemistry, Ultrafast Dynamics of the Chemical Bond, A. Zewail, (Ed.), World Scientific, Singapore, 1994, Vols. I and II.
[7] Femtosecond Chemistry, J. Manz, L. Wöste, (Eds.). VCH Verlagsgesellschaft, Weinheim, 1995, Vols. I and II.
[8] R. Weinkauf, P. Aicher, G. Wesley, J. Grotemeyer, E.W. Schlag, J. Phys. Chem. 98 (1994) 8381.
[9] K.W.D. Ledingham, R.P. Singhai, Int. J. Mass Spectrom. Ion Processes 163 (1997) 149.
[10] C. Grun, R. Heinicke, Ch. Weickhardt, J. Grotemeyer, Int. J. Mass Spectrom. 185/186/187 (1999) 307.
[11] S.M. Penn, C.C. Hayden, K.J. Carlson Muyskens, F.F. Crim, J. Chem. Phys. 89 (1988) 2902.
[12] J.F. Black, I. Powis, Chem. Phys. 125 (1988) 375.
[13] J.W. Thoman, D.W. Chandler, D.H. Parker, M.H.M. Janssen, Laser Chem. 9 (1988) 27.
[14] L.R. Khundar, A.H. Zewail, Chem. Phys. Lett. 142 (1987) 426.
[15] J.L. Knee, L.R. Kundar, A.H. Zewail, J. Chem. Phys. 82 (1985) 4715.
[16] D. Zhong, P.Y. Cheng, A.H. Zewail, J. Chem. Phys. 105, (1996) 7864.
[17] A. Gedanken, M.B. Robin, Y.Yafet, J. Chem. Phys. 76 (1982) 4798.
[18] L. Poth, Q. Zhong, J.V. Ford, A.W. Castleman, J. Chem. Phys. 109 (1998) 4791.
[19] T. Schultz, I. Fischer, J. Phys. Chem. 101 (1997) 5031.
[20] Y.-J. Jung, Y.S. Kim, W.K. Kang, K.-H. Jung, J. Chem. Phys. 107 (1997) 7187.
[21] J.W. Hepburn, D.J. Trevor, J.E. Pollard, D.A. Shirley, Y.T. Lee, J. Chem. Phys. 76 (1982) 4287.
[22] R. Weinkauf, U. Boesl, J. Chem. Phys. 98 (1992) 4459.
[23] K. Kimura, Int. Rev. Phys. Chem. 6 (1987) 195, and references therein.
[24] M. Seel, W. Domcke, J. Chem. Phys. 95 (1991) 7806.
[25] I. Fischer, D.M. Villeneuve, M.J.J. Vrakking, A. Stolow, J. Chem. Phys. 102 (1995) 5566.
[26] B. Kim, C.P. Schick, P.M. Weber, J. Chem. Phys. 103 (1995) 6903.
[27] L. Lehr, M.T. Zanni, C. Frischkorn, R. Weinkauf, D.M. Neumark, Science 284 (1999) 635.
[28] B. J. Greenblatt, M.T. Zanni, D.M. Neumark, Science 276 (1997) 1675.
[29] B. Brehm, E. von Puttkamer, Z. Naturforsch. 22a (1967) 8.
[30] W.A. Brand, T. Baer, C.E. Klots, Chem. Phys. 76 (1983) 111.
[31] V. Stert, W. Radloff, T. Freudenberg, F. Noack, I.V. Hertel, C. Jouvet, C. Delonder-Lardeux, D. Solgani, Europhys. Lett. 40 (1997) 515.
[32] W. Radloff, V. Stert, Th. Freudenberg, I.V. Hertel, C. Jouvet, C. Dedonder-Lardeux, D. Solgadi, Chem. Phys. Lett. 281 (1997) 20.
[33] P. Kruit, F. H. Read, J. Phys. E 16 (1983) 313.
[34] O. Cheshnovsky, S.H. Yang, C.L. Pettiette, M.J. Craycraft, R.E. Smalley, Rev. Sci. Instrum. 58 (1987) 2131.
[35] H. Handschuh, G. Ganteför, W. Eberhardt, Rev. Sci. Instrum. 66 (1995) 3838.
[36] R. Weinkauf, K. Walter, C. Weikhardt, U. Boesl, E.W. Schlag, Z. Naturforsch. 44a (1989) 1219.
[37] Galileo, Sturbridge MA, U.S.A. MCP data sheet.
[38] M. Tadjeddine, G. Bouchoux, L. Malegat, J. Durup, C. Pernot, J. Weiner, Chem. Phys. 69 (1982) 229.
[39] K. Walter, R. Weinkauf, U. Boesl, E.W. Schlag, J. Chem. Phys. 89 (1988) 1914.